

# Metamorphic evolution of aluminous granulites from Labwor Hills, Uganda

Michael Sandiford<sup>1</sup>, Fiona B. Neall<sup>2</sup>, and Roger Powell<sup>1</sup>

<sup>1</sup> Department of Geology, University of Melbourne, Parkville, Victoria 3052, Australia

<sup>2</sup> Department of Physical Sciences, Griffith University, Nathan, Queensland, Australia

**Abstract.** Sapphirine-cordierite-quartz and spinel-cordierite-quartz form relic assemblages of probable Archaean age in Fe-rich aluminous metapelites from Labwor Hills, Uganda, and reflect an unusually high temperature metamorphism ( $\sim 1,000^\circ\text{C}$ ) at pressures in the vicinity of 7–9 kbars and  $a(\text{O}_2)$  near the magnetite-hematite buffer. Subsequent reaction textures include the replacement of spinel and cordierite by sillimanite and hypersthene and formation of sapphirine-hypersthene-K-feldspar-quartz symplectites which are interpreted as pseudomorphs after osumilite. A petrogenetic grid appropriate to these assemblages suggests these reaction textures may be due to cooling at constant or increasing pressure and constant  $a(\text{O}_2)$ , or decreasing  $a(\text{O}_2)$  at constant temperature and pressure. The former interpretation is supported by the coexistence of ilmenohematite and magnetite during the development of the reaction textures, and by the comparatively low  $\text{Al}_2\text{O}_3$ -contents of secondary hypersthene. This pressure-temperature path implies that: (1) metamorphism occurred at deep levels within normal thickness crust, probably less than 40–45 km thick, due to an extreme thermal perturbation induced either by emplacement of mantle-derived magmas or by thinning of the subcontinental lithosphere in an extensional tectonic regime, (2) the excavation and surface exposure of the granulites is due to a subsequent, postgranulite facies metamorphism, crustal thickening most probably involving their incorporation into an allochthonous upper crustal thrust sheet during the formation of the Mozambique fold-belt.

## Introduction

Sapphirine granulites commonly preserve textural evidence for retrograde reaction in the form of corona and symplectite development (Morse and Talley 1971; Sheraton et al. 1980; Warren 1983; Droop and Bucher-Nurminen 1984; Sandiford 1985). These reaction textures are particularly useful in the elucidation of retrograde pressure-temperature paths and, therefore, may provide important insights into the tectonic setting of metamorphism (Thompson 1981). In this paper we describe assemblages and reaction textures in Precambrian (probably Archaean) granulites from the Labwor Hills in Uganda. These assemblages provide new

insights into the phase relationships in aluminous granulites at high temperatures, while the reaction textures, which include the unusual symplectite assemblage sapphirine-hypersthene-K-feldspar-quartz believed to derive from prograde osumilite, indicate retrograde cooling from very high temperatures at constant or increasing pressure. In this paper we discuss constraints on this pressure-temperature path and its implications for the tectonic evolution of the Labwor Hills granulites.

## Geological setting

The Labwor Hills granulites form part of an extensive high grade metamorphic terrain in northern Uganda bounded to the southwest by the Aswa mylonite belt (Baldrock et al. 1969), and to the east by the Mozambique foldbelt (Shackleton 1986). Together with a number of other small granulite bodies in Northern Uganda, the Labwor Hills granulites are believed to be relics of an Archaean metamorphic terrain (Clifford 1975). The unusual nature of the Labwor Hills granulites was highlighted by Nixon et al. (1973) who reported the occurrence of sapphirine-quartz assemblages, then only known from two other terrains (Dallwitz 1968; Morse and Talley 1971), and subsequently by Nixon et al. (1984) who reported kornerupine. Nixon et al. (1973) suggested these granulites crystallised at unusually hot temperatures, possibly as high as  $1,050^\circ\text{C}$ ; a suggestion which receives considerable support from the work presented here. Most subsequent reviews of the pressure-temperature field of granulite facies metamorphism have included the Labwor Hills as the hottest known granulites (Newton and Perkins 1982; Harley 1984).

The rocks described herein are from Nixon's original collection. The field relationship between the individual samples is poorly known. However sapphirine granulites are confined to an area approximately 20 square miles in area with a distinctive foliation trend (Nixon et al. 1973), and as all the rocks described herein show evidence for an unusually high temperature metamorphism followed by an equally unusual and distinctive cooling history, the assumption of a common tectonic evolution is believed to be valid.

## Petrography

Twelve samples have been investigated in this study. They include a variety of aluminous rocks derived most probably from ferruginous pelites. Minerals present and a summary of the textural relationships in each of the samples are listed in Table 1. The general petrographic features of these rocks are summarised below.

The extraordinary diversity of mineral associations in the individual samples (Table 1) reflects the very complex

**Table 1.** Summary of textural relationships in the Labwor Hills granulites

	4799	4800	4801	4802	4803	4804	4805	4806	4807	4808	4809	4810
Quartz	R	P R <sub>3</sub>	P	P	P R <sub>3</sub>	P	P	R <sub>3</sub>	P	P	P R <sub>3</sub>	P R <sub>3</sub>
Plagioclase		P		P	P		P			P	P	P
K-feldspar		R <sub>3</sub>	R <sub>5</sub>		R <sub>3</sub>			R <sub>3</sub>			R <sub>3</sub>	R <sub>3</sub>
Osumilite <sup>a</sup>		P			P			P			P	P
Garnet	R <sub>2</sub>	P R <sub>2</sub>		R <sub>2,5,6</sub>		R <sub>2,6,7</sub>					R <sub>2,6,7</sub>	R <sub>2,6,7</sub>
Hypersthene	P	P R <sub>3</sub>	R <sub>4,10</sub>	P <sub>?</sub> R <sub>10</sub>	P <sub>?</sub> R <sub>3,10</sub>	P <sub>?</sub> R <sub>10</sub>	R <sub>4,10</sub>	P <sub>?</sub> R <sub>3,10</sub>		R <sub>9,10</sub>	R <sub>3,10</sub>	R <sub>3,10</sub>
Sapphirine		R <sub>2,3</sub>	R <sub>2</sub>		R <sub>2,3,5,6</sub>	R <sub>2</sub>	R <sub>2,7</sub>	P <sub>?</sub> R <sub>3</sub>	R	P R <sub>6,7</sub>	R <sub>2,6,7</sub>	R <sub>2,6,7</sub>
Cordierite			P	P		P	P		P	P	P	P
Sillimanite	R		R <sub>2,4,5,6</sub>	R <sub>2,5,6</sub>	R <sub>5,6</sub>	P <sub>2,4,5,6</sub>	R <sub>2,4,6,7</sub>	R <sub>2,6,7</sub>	R <sub>4</sub>	R <sub>2,6,7,9</sub>	R <sub>2,4,6,7</sub>	R <sub>2,4,6,7</sub>
Corundum									P <sub>?</sub> <sub>8</sub>			P
Spinel	P	P	P	P	P	P	P	P	P	P	P	P
Magnetite	P	P	P	P	P	P	P	P	P	P	P	P
Hematite	P	P	P	P	P	P	P	P	P	P	P	P
Ilmenite	R <sub>1</sub>	R <sub>1</sub>	R <sub>1</sub>	R <sub>1</sub>	R <sub>1</sub>	R <sub>1</sub>	R <sub>1</sub>	R <sub>1</sub>	R <sub>1</sub>	R <sub>1</sub>	R <sub>1</sub>	R <sub>1</sub>
Biotite		R		R		R	R		R	R	R	

<sup>a</sup> osumilite does not occur in these rocks but its former presence is indicated on textural grounds (see text)

P interpreted to have been stable as part of the highest grade (prograde) mineral assemblage

R interpreted to have formed during retrograde cooling

? ambiguous textural relations preclude definitive assignment to P or R, respectively

1 as exsolution lamellae in hematite; 2 as coronas on spinel; 3 as part of the symplectite developed as a pseudomorph after osumilite; 4 as a replacement of cordierite; 5 intergrown with cordierite; 6 as coronas on magnetite; 7 as coronas on hematite; 8 in quartz-absent domains only; 9 as coronas on sapphirine; 10 as part of the retrograde sillimanite-producing textures

**Fig. 1.** Photomicrograph of 4803, illustrating the existence of an early formed coarse grained equilibrated texture between three phases including hypersthene (*hy*) and quartz (*q*). The third phase, (*o*), has been subsequently pseudomorphed by a fine grained symplectite composed of sapphirine, orthopyroxene, K feldspar and quartz (see Fig. 7). This pseudomorphed phase is believed to have been osumilite. Field of view is approximately 2 × 3 mm

**Fig. 2.** Backscattered SEM image depicting the coarse grained granoblastic fabric in 4799 defined by hypersthene (*hy*) and spinel (*sp*) which are interpreted to have formed part of a stable prograde assemblage. Subsequent reaction has resulted in the exsolution of lamellae and blebs of magnetite (*m*) from spinel, and the formation of garnet (*g*) coronas around spinel. Elsewhere the garnet coronas have inclusions of quartz and sillimanite. Field of view is approximately 0.8 × 1.2 mm

**Fig. 3.** Optical photomicrograph showing reaction between spinel (*sp*) and cordierite (*cd*) giving sillimanite and hypersthene (*hy*) in 4801. The primary assemblage in this sample is inferred to have included cordierite, spinel, quartz, hematite and, possibly, osumilite and magnetite. Field of view is approximately 1.0 × 1.5 mm

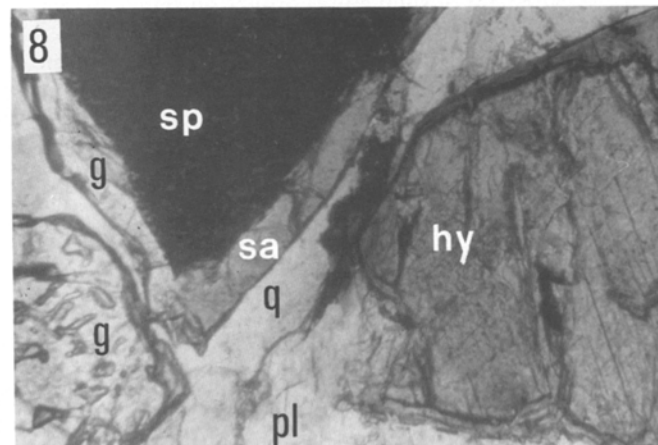
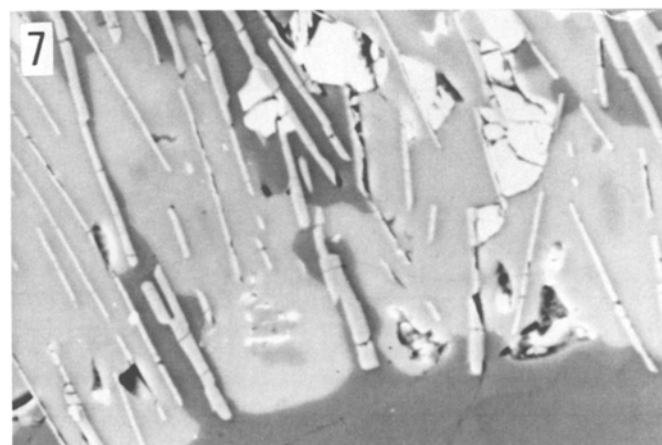
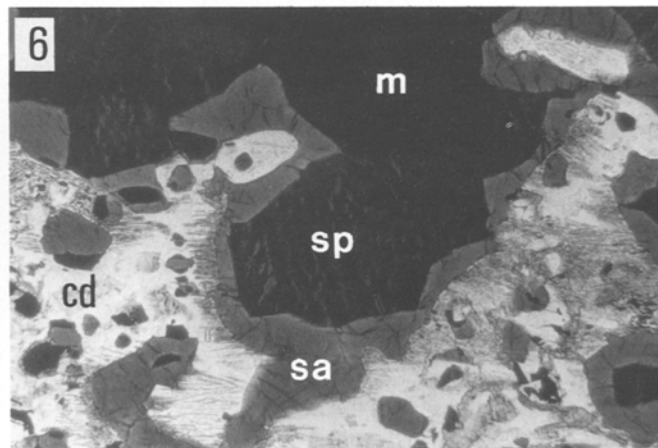
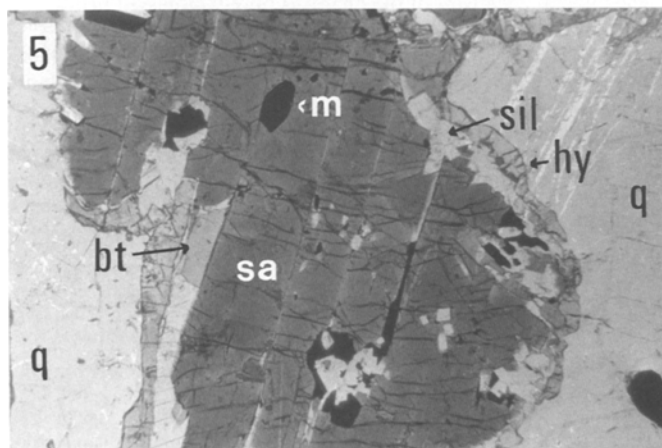
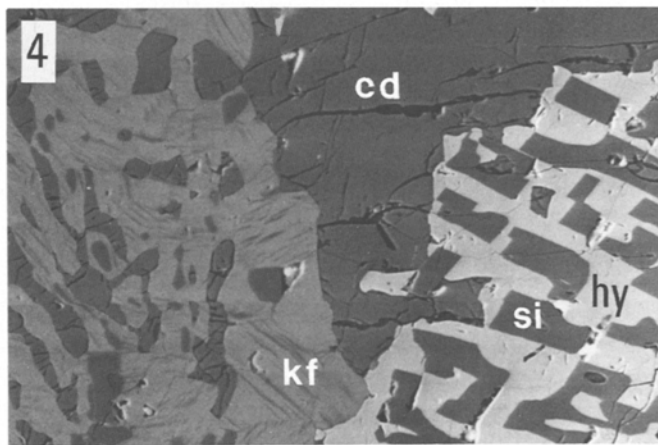
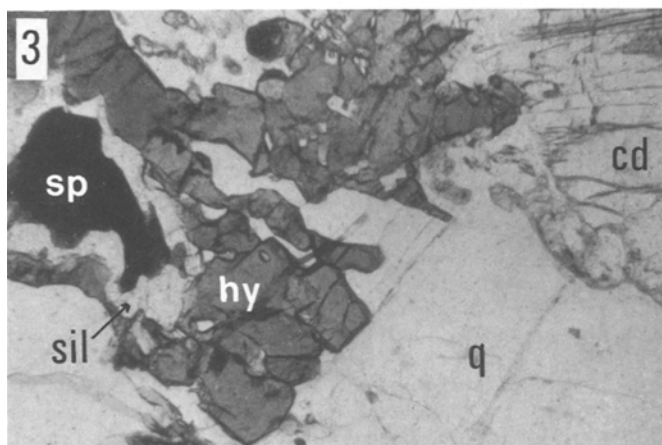
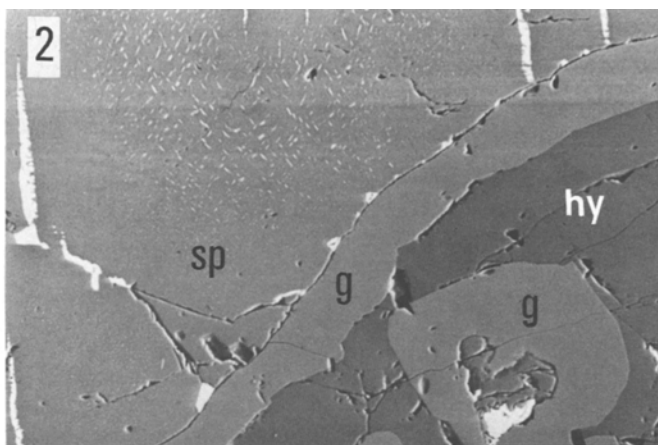
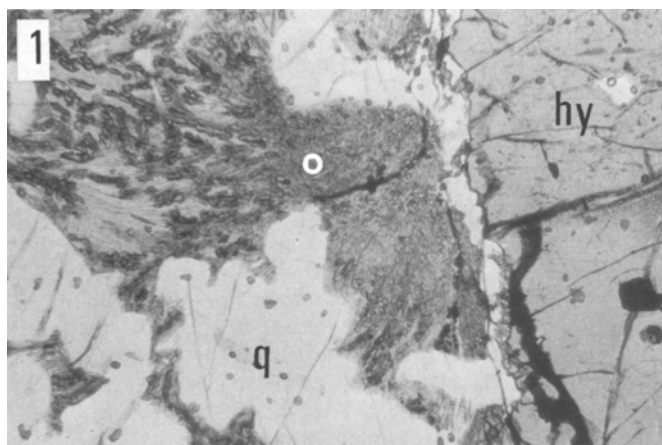
**Fig. 4.** Backscattered SEM image showing detail of reaction rims on cordierite (*cd*) in 4801. The large cordierite grain, which is extensively twinned, is partially replaced by sillimanite and hypersthene (*hy*) where it abuts coarse grained spinel (see Fig. 3). Elsewhere the large cordierite cores are rimmed by fine grained intergrowths of cordierite and K-feldspar (*Kf*). The cordierite intergrown with K-feldspar is optically continuous with individual twin lamellae in the large cordierite grain, implying replacement of cordierite by K-feldspar. This texture may reflect reaction involving primary osumilite, however, the diagnostic breakdown products of osumilite (see Figs. 1 and 7) have not been recorded in this sample. Field of view is approximately 0.6 × 0.9 mm

**Fig. 5.** Optical photomicrograph showing rims of sillimanite (*sil*) and hypersthene (*hy*) between primary sapphirine (*sa*) and quartz (*q*) in sample 4808. Additional phases include magnetite (*m*) and biotite (*bt*). Field of view is approximately 1.4 × 2.0 mm

**Fig. 6.** Optical photomicrograph showing the development of sapphirine (*sa*) rims on spinel (*sp*) and magnetite (*m*) in cordierite-bearing rock (4810). Sapphirine also occurs as thin aligned blades in a matrix of quartz and feldspar adjacent to cordierite. Field of view is approximately 1.6 × 2.4 mm

**Fig. 7.** Backscattered SEM image showing details of sapphirine-hypersthene-K feldspar-quartz symplectite in 4803 (see also Fig. 1). Sapphirine is the high relief, intermediate contrast, bladed phase. Hypersthene is the lightest contrast phase occurring as high relief blebs. K-feldspar is the intermediate contrast, low relief phase. Quartz is the darkest contrast, low relief phase. These intergrowths are believed to represent the breakdown of osumilite which formed part of the early formed assemblage osumilite-hypersthene-quartz-plagioclase-spinel-magnetite-hematite. Field of view is approximately 0.14 × 0.2 mm

**Fig. 8.** Optical photomicrograph showing secondary rims of sapphirine (*sa*) and garnet (*g*) on spinel (*sp*) in 4805. Spinel formed part of the early formed assemblage with quartz (*q*), plagioclase (*p*), hypersthene (*hy*), magnetite, hematite and cordierite. Field of view is approximately 0.6 × 0.9 mm



textural evolution of these rocks. Each sample has numerous reaction textures involving a variety of phases with the total number of phases generally being considerable. For instance, samples 4809 and 4810 each contain thirteen phases. This diversity of mineral associations is attributed to a succession of reactions developed between large mineral grains formed at an early stage in the metamorphic history. In the texturally least complex samples, these coarse grained phases can be recognised as having formed part of an equilibrated polygonal texture during this early 'event'. Progressive textural complexity is marked by the development of fine-grained intergrowths along the grain boundaries of the early texture, the pseudomorphous replacement of components of the early texture by symplectites (Fig. 1), and finally by the complete masking of the early texture by a morass of finely intergrown reaction products. Phases identified as forming part of these early texturally equilibrated assemblages define a distinct, probably prograde, metamorphic association. The following assemblages have been inferred (Table 1):

orthopyroxene-spinel-ilmenohematite-(magnetite)

garnet-spinel-hypersthene-plagioclase-quartz-ilmenohematite-osumilite-(magnetite).

cordierite-spinel-hypersthene-plagioclase-quartz-ilmenohematite-osumilite-(magnetite)

sapphirine-cordierite-spinel-plagioclase-quartz-ilmenohematite-magnetite)

Fresh osumilite is not preserved in any of the rocks investigated and its former presence as a member of the above assemblages is based on the interpretation of an unusual reaction texture discussed at length in a following section. The petrographic observations bearing on the oxide phase relationships at peak temperatures, particularly the coexistence of spinel and magnetite, are discussed below.

Reaction textures developed subsequently in these early formed assemblages include:

1. the rimming of hypersthene and spinel by garnet, sillimanite and quartz (Fig. 2);
2. the partial or complete replacement of cordierite by sillimanite and hypersthene (Figs. 3 and 4);
3. the development of hypersthene-sillimanite coronas between spinel and quartz, and sapphirine and quartz (Figs. 3 and 5);
4. development of sapphirine coronas on spinel, magnetite and ilmenohematite (Fig. 6);
5. the development of sillimanite coronas on spinel, magnetite and ilmenohematite;
6. the development of a symplectite consisting of sapphirine, hypersthene, quartz and K-feldspar (see later discussion, Figs. 1 and 7);
7. the development of sapphirine and garnet between primary spinel and hypersthene (Fig. 8);
8. the development of biotite sheaths around ilmenohematite and magnetite.

The relationships between the oxide phases is critical to the petrogenetic model for the silicate reaction textures presented in this paper. All samples contain four oxide phases; spinel-hercynite solid solution (termed here spinel), magnetite, hematite and ilmenite. Rutile, which has been recorded from Labwor Hills by Nixon et al. (1973), is not present in the samples described here. Hematite and ilmenite

occur as intergrown lamellae with hematite typically more abundant than ilmenite, suggesting that ilmenohematite formed part of the early-formed equilibrated texture. In some samples the primary Fe—Ti-oxide may have been hemoilmenite (see Nixon et al. 1973); Fe—Ti substitution appears to have been in excess of the hematite-ilmenite solvus during this stage. Both spinel and magnetite occur as coarse-grained polygonal phases. Spinel contains exsolution lamellae of magnetite, and magnetite contains exsolution blebs of spinel and lamellae of ilmenite. Thus, the textural relationships suggest that both spinel and Ti-magnetite occurred as discrete phases at peak temperatures, albeit with substantial mutual solid solution. However, the relevant experimental data (Lindsley 1976) suggests complete closure of the spinel-magnetite solvus at the temperatures of peak metamorphism which we estimate to have been  $\sim 1,000^\circ\text{C}$  (see later discussion) and therefore it is possible that apparently stable polygonal intergrowths of spinel and magnetite have originated as a product of granule exsolution during cooling. If this is the correct interpretation, exsolution must have predated the development of the silicate reaction textures described above, which are equally well developed on magnetite and spinel.

## Mineral chemistry

Representative electron microprobe analyses of the principal Fe—Mg phases present in the Labwor Hills granulites are presented in Tables 2–6. Analyses were performed on the Cambridge University, Department of Earth Science instrument at 20 kV accelerating potential and the JEOL-JX5A microprobe at the Department of Geology, University of Melbourne at 15 kV accelerating potential. The mineral chemistry of the phases is briefly discussed below.

*Garnet*, Table 2, forming part of the primary assemblage (4800) and forming secondary coronas between hypersthene and spinel (4799 and 4802), is essentially a solid solution midway between almandine and pyrope, with  $X_{\text{Fe}} = 0.47\text{--}0.55$  (where  $X_{\text{Fe}} = \text{Fe}^{2+}/\text{Fe}^{2+} + \text{Mg}$ ). Very low ferric iron contents are suggested by octahedral Al site occupancy close to the theoretical maximum, within

**Table 2.** Electron microprobe analyses of garnet. Structural formulae have been calculated on the basis of 12 oxygens

	4799 <sup>c</sup>	4800 <sup>a</sup>	4800 <sup>b</sup>	4800 <sup>c</sup>	4802 <sup>c</sup>
SiO <sub>2</sub>	39.29	39.57	39.38	39.75	39.77
Al <sub>2</sub> O <sub>3</sub>	22.38	22.62	22.45	23.04	22.32
FeO	24.96	21.13	23.17	23.58	25.08
MnO	1.22	1.52	1.53	1.40	0.59
MgO	11.90	13.47	12.41	12.57	11.51
CaO	0.25	1.07	0.86	0.82	1.60
Total	100.00	99.38	99.80	101.16	100.87
Si	2.983	2.980	2.980	2.967	2.995
Al	2.003	2.009	2.003	2.028	1.982
Fe	1.585	1.331	1.467	1.472	1.580
Mn	0.079	0.097	0.098	0.089	0.038
Mg	1.346	1.512	1.399	1.398	1.292
Ca	0.020	0.086	0.069	0.066	0.129
Fe/Fe + Mg	0.54	0.47	0.51	0.51	0.55

<sup>a</sup> core analysis of prograde garnet

<sup>b</sup> rim analysis of prograde garnet

<sup>c</sup> analysis of retrograde garnet corona

**Table 3.** Electron microprobe analyses of sapphirine. DHZ21 represents the Labwor Hills sapphirine analysis of Sahama et al. (1974), quoted by Deer et al. (1978). Structural formula have been calculated on the basis of 10 oxygens with  $\text{Fe}^{3+}$  determined by balancing charges

	4800 <sup>b</sup>	4803 <sup>b</sup>	4806 <sup>b</sup>	4808 <sup>a</sup>	DHZ21
$\text{SiO}_2$	12.51	13.20	13.75	13.43	13.76
$\text{Al}_2\text{O}_3$	61.72	59.41	56.54	56.63	57.21
FeO	9.69	11.87	14.28	13.22	12.36
MnO	0.07	0.28	0.40	0.41	0.35
MgO	15.91	15.27	14.65	15.74	14.73
$\text{Cr}_2\text{O}_3$	0.38	0.21	—	0.12	—
Total	100.28	100.24	99.62	99.55	98.41
Si	0.742	0.794	0.841	0.816	0.847
Cr	0.018	0.010	—	0.006	—
Al	4.316	4.215	4.074	4.057	4.143
$\text{Fe}^{3+}$	0.116	0.187	0.244	0.303	0.153
$\text{Fe}^{2+}$	0.365	0.411	0.485	0.369	0.483
Mn	0.004	0.014	0.021	0.021	0.018
Mg	1.406	1.369	1.335	1.426	1.351
$\text{Fe}^{2+}/\text{Mg} + \text{Fe}^{2+}$	0.21	0.23	0.26	0.21	0.26
$\text{Fe}^{3+}/\text{Fe}^{2+} + \text{Fe}^{3+}$	0.26	0.31	0.34	0.45	0.24

<sup>a</sup> core analysis of prograde sapphirine

<sup>b</sup> analysis of retrograde sapphirine corona

**Table 4.** Electron microprobe analyses of orthopyroxene. Structural formula have been calculated on the basis of 6 oxygens with  $\text{Fe}^{3+}$  determined by balancing charges

	4799 <sup>a</sup>	4799 <sup>b</sup>	4800 <sup>a</sup>	4802 <sup>a</sup>	4803 <sup>a</sup>	4808 <sup>c</sup>
$\text{SiO}_2$	49.36	49.75	47.93	49.61	46.68	49.98
$\text{TiO}_2$	0.09	0.17	0.18	na	na	na
$\text{Al}_2\text{O}_3$	7.57	6.45	10.74	7.71	11.83	7.05
FeO	19.52	19.28	18.27	20.58	19.87	18.87
MnO	0.26	0.23	0.33	0.24	0.81	1.10
MgO	23.44	24.67	23.07	23.82	20.92	23.27
CaO	—	—	0.06	0.10	0.11	—
Total	100.24	100.55	100.58	102.06	100.22	100.27
Si	1.798	1.800	1.731	1.774	1.709	1.823
Ti	0.003	0.005	0.005	0.004	—	—
Al	0.325	0.275	0.457	0.325	0.511	0.303
$\text{Fe}^{3+}$	0.075	0.116	0.070	0.118	0.070	0.052
$\text{Fe}^{2+}$	0.520	0.467	0.482	0.497	0.538	0.524
Mn	0.008	0.007	0.010	0.007	0.025	0.034
Mg	1.272	1.330	1.242	1.270	1.142	1.264
Ca	—	—	0.002	0.004	0.004	—
$\text{Fe}^{2+}/\text{Mg} + \text{Fe}^{2+}$	0.29	0.26	0.28	0.28	0.32	0.29
$\text{Fe}^{3+}/\text{Fe}^{2+} + \text{Fe}^{3+}$	0.13	0.20	0.13	0.19	0.12	0.09

<sup>a</sup> core analysis of prograde orthopyroxene

<sup>b</sup> rim analysis of prograde orthopyroxene

<sup>c</sup> analysis of retrograde orthopyroxene corona

analytical error. Grossular and spessartine molecules comprise less than 5 molecular% of both prograde and retrograde garnets. In 4800, garnet rims are significantly enriched in almandine component with respect to the core.

**Table 5.** Electron microprobe analyses of cordierite. Structural formula have been calculated on the basis of 18 oxygens.  $\text{Fe}^{3+}$  has been determined by balancing charges, assuming an anhydrous composition

	4800 <sup>a</sup>	4801 <sup>a</sup>	4804 <sup>a</sup>
$\text{SiO}_2$	49.81	49.88	50.00
$\text{Al}_2\text{O}_3$	34.12	34.17	33.82
FeO	1.99	3.23	3.67
MnO	—	—	0.12
MgO	12.33	11.47	11.12
Total	98.25	98.75	98.73
Si	4.978	4.989	5.013
Al	4.020	4.029	3.997
$\text{Fe}^{3+}$	0.025	—	—
$\text{Fe}^{2+}$	0.141	0.270	0.307
Mn	—	—	—
Mg	1.836	1.709	1.661
$\text{Fe}^{2+}/\text{Mg} + \text{Fe}^{2+}$	0.07	0.14	0.16

<sup>a</sup> core analysis of prograde cordierite

**Table 6.** Electron microprobe analyses of spinel and magnetite. Structural formula have been calculated on the basis of 4 oxygens with  $\text{Fe}^{3+}$  determined by balancing charges

	4799 <sup>a</sup>	4799 <sup>b</sup>	4799 <sup>a</sup>	4800 <sup>a</sup>	4801 <sup>a</sup>	4805 <sup>a</sup>	4809 <sup>a</sup>
$\text{SiO}_2$	0.14	—	0.06	0.07	0.11	0.49	0.58
$\text{TiO}_2$	—	0.07	0.11	0.07	0.00	—	—
$\text{Al}_2\text{O}_3$	59.44	59.49	0.27	61.30	60.15	58.81	63.76
FeO	28.16	28.12	90.56	24.42	25.71	30.35	21.97
MnO	0.14	0.14	0.06	0.14	0.36	0.22	0.27
MgO	11.59	11.95	—	13.32	12.08	9.65	11.96
$\text{Cr}_2\text{O}_3$	0.76	0.84	0.58	1.02	0.48	0.21	0.34
Total	100.23	100.61	91.64	100.34	98.89	99.73	98.88
Si	0.004	—	0.001	0.002	0.003	0.013	0.016
Ti	—	0.002	0.001	0.002	0.003	0.013	0.016
Cr	0.016	0.018	0.018	0.001	0.010	0.005	0.006
Al	1.882	1.887	0.012	0.021	1.912	1.892	1.988
$\text{Fe}^{3+}$	0.095	0.092	1.959	0.064	0.071	0.077	—
$\text{Fe}^{2+}$	0.537	0.519	1.004	0.476	0.508	0.616	0.486
Mn	0.003	0.003	—	0.003	0.008	0.05	0.006
Mg	0.464	0.479	—	0.524	0.485	0.392	0.472
$\text{Fe}^{2+}/\text{Mg} + \text{Fe}^{2+}$	0.54	0.52	—	0.48	0.51	0.61	0.51
$\text{Fe}^{3+}/\text{Fe}^{2+} + \text{Fe}^{3+}$	0.15	0.15	0.66	0.12	0.12	0.11	—

<sup>a</sup> core analysis of prograde spinel/magnetite

<sup>b</sup> rim analysis of prograde spinel

*Sapphirine*, Table 3, in the Labwor Hills granulites is amongst the most Fe-rich reported (see also Sahama et al. 1974; Deer et al. 1978). Exceptionally high ferric iron contents have been reported by Sahama et al. (1974) and similarly high ferric iron contents in the sapphirines reported here are suspected on the basis of charge balance. Calculating ferric iron by balancing charges yields structural formulae with  $\text{R}^{2+}:\text{R}^{3+}:\text{R}^{4+}$ ; between 2:3:1 and 7:9:3. It is however noteworthy that the wet chemical analyses provided by Sahama et al. (1974) reveal substantially more ferric iron than estimated by charge balance (Table 3), and consequently determi-

nation of ferric iron on the basis of charge balance in sapphirines appears to be subject to some inaccuracy.

*Hypersthene* (Table 4) with  $X_{Fe}=0.26-0.32$  is characterised by very high  $Al_2O_3$  contents, especially in the cores of prograde grains which have  $Al^{VI}=0.10-0.20$ . Ferric/ferrous ratios determined by balancing charges are substantially lower than coexisting sapphirine but equivalent to or greater than coexisting spinel. Retrograde hypersthene in coronas and symplectites is characterised by significantly lower  $Al_2O_3$  and marginally lower  $X_{Fe}$  compared with cores of prograde hypersthene.

*Cordierite* (Table 5) is enriched in magnesium with respect to all other coexisting Fe–Mg bearing phases, with the analysed cordierites yielding  $X_{Fe}=0.07-0.16$ . In all specimens cordierite shows spectacular multiple twinning, suggesting that it may have undergone the ordering transition associated with the hexagonal-orthorhombic transformation (Putnis and Holland 1986). However the sector twinning diagnostic of such transformations has not been identified and the twinning may simply be a consequence of deformation.

*Spinel* (Table 6) is essentially a hercynite-spinel solid solution with  $X_{Fe}=0.48-0.61$ . Spinel is fractionally more enriched in magnesium with respect to iron than coexisting garnet and less magnesian than coexisting hypersthene. The ferric iron content of spinels determined by balancing charges is significantly lower than coexisting sapphirine. However, as all analysed spinels contain appreciable magnetite as exsolution lamellae and blebs, the equilibrium spinel composition during peak metamorphism must have been considerably more Fe-rich and must have had a greater proportion of ferric iron. Consequently, the relative partitioning of ferric and ferrous iron and ferrous iron and magnesium between spinel and coexisting phases at peak conditions is problematical. The analysed spinels have low chromium contents and zinc was not detectable.

### Evidence for osumilite

Theoretical studies suggest that osumilite should be an important phase during granulite metamorphism because it replaces K-feldspar in pelitic assemblages at temperatures in excess of  $900-1,000^\circ C$  at pressures below about 8–11 kbar (Hensen 1977; Ellis et al. 1980; Grew 1982). However, osumilite has only been reported from a few very high grade metamorphic terrains (Berg and Wheeler 1976; Majer et al. 1977; Bogdanova et al. 1980; Ellis et al. 1980). One reason for its apparent scarcity in granulite terrains is that osumilite appears to breakdown readily during cooling. In the Napier Complex granulites from Antarctica osumilite is invariably replaced by fine grained symplectites of cordierite, K-feldspar, quartz and hypersthene (Ellis et al. 1980; Grew 1982). Indeed similar cordierite-K-feldspar-quartz symplectites from Rogaland in Norway, Wilson Lake in Canada, and Paderu in Southern India have been argued to represent osumilite breakdown products (Schreyer and Seifert 1967; Grew 1982). Similarly we suggest that the sapphirine-hypersthene-K-feldspar-quartz symplectite in the Labwor Hills granulites represents an osumilite breakdown texture. Importantly, this assemblage is chemically equivalent to cordierite-hypersthene-K-feldspar-quartz, differing only from osumilite in being slightly enriched in iron with respect to magnesium (Fig. 9), which suggests that breakdown of osumilite represents a continuous reaction in the divariant assemblage; its textural occurrence in the Labwor granulites suggests that it forms a pseudomorph after a phase forming part of the early coarse-grained fabric.

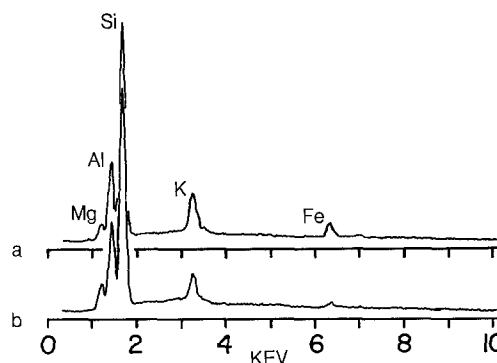


**Fig. 9a, b.** Energy dispersive spectra for Labwor Hills sapphirine-orthopyroxene-K feldspar-quartz symplectite in 4803 (a) and for osumilite from Brusilov Nunataks, Enderby Land, Antarctica (b). The symplectite composition differs only slightly from the Antarctic osumilite; containing more Fe and K and less Mg and Al on a Si-equivalent basis. X-ray energy for individual peaks is as follows;  $Mg_{K\alpha}=1.28$  KeV;  $Al_{K\alpha}=1.4$  KeV;  $Si_{K\alpha}=1.75$  KeV;  $K_{K\alpha}=2.35$  KeV;  $Fe_{K\alpha}=6.4$  KeV. The Antarctic osumilite has the composition  $(K_{0.9}Na_{0.1})(Fe_{0.5}Mg_{1.9})Al_{3.6}Si_{10}O_{30}$  (Grew 1982)

### A petrogenetic grid appropriate to the Labwor Hills granulites

The inferred prograde assemblages and retrograde reaction textures in the Labwor Hills granulites may be used to constrain the topology of the  $FeO-MgO-Al_2O_3-TiO_2-SiO_2-O_2$  (FMAS<sub>TO</sub>) system involving the phases garnet, spinel, hypersthene, sapphirine, cordierite, sillimanite, quartz, magnetite, and hematite, and the  $K_2O-FeO-MgO-Al_2O_3-SiO_2-TiO_2-O_2$  (KFMA<sub>STO</sub>) system involving the additional phases osumilite and K-feldspar (Fig. 10).  $TiO_2$  is included in the system because the Labwor Hills oxide phases are believed to have contained significant solid solution with Ti-phases at peak metamorphism.

The diagnostic prograde assemblages are osumilite-cordierite-spinel-hypersthene-quartz and sapphirine-spinel-cordierite-quartz. Importantly, prograde garnet does not occur with cordierite and is restricted to plagioclase-bearing assemblages suggesting it may have only been stable in bulk compositions with appreciable CaO. In view of these considerations and the presence of reaction textures involving sillimanite and hypersthene after spinel-cordierite-sapphirine-quartz assemblages, the garnet-absent invariant point, [g], is considered a stable part of the FMAS<sub>TO</sub> topology. In accordance with Hensen (1986), the additional invariant points [sa] and [cd] are also considered stable, while [sil], [hy] and [sp] are considered metastable. The petrogenetic grid presented in Fig. 10 is topologically identical to that of Hensen (1986), however the significance of the reaction boundaries is somewhat different. In the presence of hematite and magnetite, our FMAS<sub>TO</sub> grid is independent of  $a(O_2)$ , and consequently the reaction lines represent true univariant reactions. In Hensen's grid the reaction lines represent divariant reactions (or iso- $a(O_2)$  univariants). At  $a(O_2)$  lower than that required to stabilise hematite, the grid will contract along the metastable extension of the hematite-absent univariants (shown as dashed lines in Fig. 10). The invariant point [hem] therefore has a unique significance, representing a point of inversion between the high  $a(O_2)$  topology shown in Fig. 10 and a low  $a(O_2)$  topology involving the stable invariant points [sp], [sil] and [hy] (Hensen 1971, 1986).





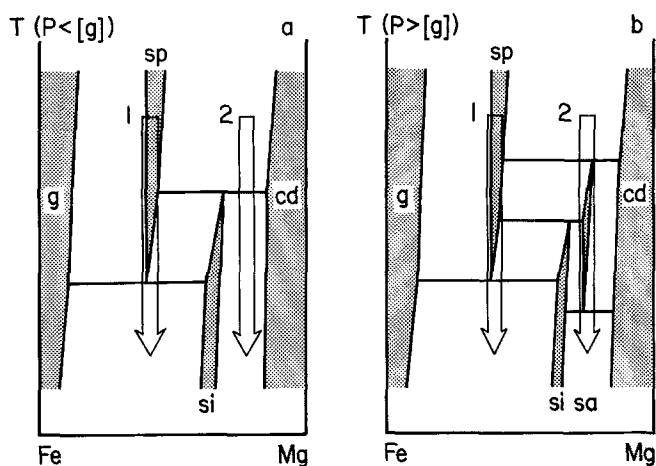


Fig. 11a, b. PT-X diagrams for the Labwor Hills hypersthene-quartz-magnetite-hematite-bearing assemblages. These diagrams represent PT sections parallel to the arrow in Fig. 10, with **a** representing a PT path for pressures less than [g], and **b** representing a path for pressures greater than [g]. Reaction textures developed in Fe-rich and Mg-rich bulk compositions (eg 4799 and 4801) are predicted by arrows 1 and 2, respectively (see text for discussion)

has seen only the (cd, sa) reaction, indicating reaction was initiated at somewhat lower temperature than the initial reaction textures in the more Mg-rich sample 4801 (Fig. 11). A number of the reaction textures involving garnet cannot be explained by the reaction path indicated in Fig. 10 (see Fig. 8). These are attributed to reactions involving plagioclase and thus cannot be considered on the FMASTO and KFMASSTO grids, but they are also consistent with formation due to cooling at constant or increasing pressures in the vicinity of 7–9 kbars.

### Tectonic implications

Pressure-temperature paths involving substantial near isobaric cooling from extremely high temperatures ( $\sim 850$ – $1,000^\circ\text{C}$ ) have been inferred in a number of high grade terrains (e.g. Ellis 1980; Ellis and Green 1985; Harley 1985; Morse and Talley 1971; Sandiford 1985; Warren 1983). In these high temperature, regional scale metamorphic terrains, such pressure-temperature paths provide a number of important constraints on the tectonic environment of metamorphism (Sandiford 1985), in particular they imply that: 1. metamorphism was induced by a transient thermal perturbation capable of providing extreme temperatures in the lower crust, 2. peak metamorphic conditions attained at mid to deep crustal levels in a crust of moderate thickness, and 3. excavation of the metamorphic terrain cannot be regarded as a consequence of the prograde tectonic cycle.

Evidence that the Archaean continental lithosphere was as thick as the modern day lithosphere (Richardson et al. 1984; England and Bickle 1984) supports the notion that the thermal and mechanical character of Archaean continental crust was similar to modern day continental crust. Consequently metamorphic temperatures of  $\sim 1,000^\circ\text{C}$  must represent significant departures from the steady state continental geotherm even for Archaean terrains. Without undue thickening of the crust, such thermal perturbations

must result from a very substantial increase in the convective and/or conductive heat input from the mantle. Very large volumes of high temperature ( $\geq 1,000^\circ\text{C}$ ) melts intruded on a large scale are required to generate such temperatures on a regional scale. Evidence for such a process in the geological record is witnessed by the occurrence of a number of the world's osunilite localities within regional scale contact aureoles around anorthosites (Berg and Wheeler 1976; Majer et al. 1977). Thermal models of magmatic arcs suggest that the temperatures in the vicinity of  $800$ – $900^\circ\text{C}$  may be attained at mid to deep crustal levels at Andean-style plate margins and the documentation of granulite facies assemblages in fossil arcs (Bard 1983; Coward et al. 1982) testifies to the relevance of these models. An alternative mechanism for generating very high temperatures within the crust involves large scale extension, where extension is either accompanied by magmatic additions from the mantle or where extensional strain is accommodated largely within the subcrustal lithosphere (Sandiford and Powell 1986a). Heat flow studies within the Basin and Range Province (Lachenbruch and Sass 1978) suggest that temperatures may reach as high as  $900^\circ\text{C}$  at depths of 30–35 km over large areas, and locally as high as  $1,000^\circ\text{C}$  at 25–30 km in places such as the Battle Mountain High, supporting the notion that high temperature granulite facies metamorphism may accompany continental extension.

Metamorphism of the Labwor Hills granulites is argued to be a consequence of an extreme thermal perturbation, with the retrograde history reflecting the waning temperatures during the decay of this thermal anomaly. During this interval of isobaric cooling the granulites are estimated to have been at depth equivalents of  $\sim 7$ – $9$  kbars ( $\sim 25$ – $30$  km). The lack of erosion implied by this isobaric cooling suggests total crustal thickness at this time was not excessive, and, by analogy with modern day continental crust with no significant erosion potential, was probably less than 40–45 km thick. The excavation of the granulites must therefore be due to a subsequent crustal thickening event, causally unrelated to the prograde tectonic cycle. The occurrence of the Labwor granulites between the Aswa mylonite zone and the boundary of the Mozambique foldbelt suggests that excavation was related to Pan African-aged foreland thickening, most probably in an imbricate thrust system (Shackleton 1986). This final point is important in deciphering the geological significance of very high temperature isobarically-cooled granulite terrains metamorphosed near the base of the continental crust, as it implies that their surface exposure requires their fortuitous incorporation into an upper crustal allochthon. The scarcity of these high temperature terrains in the geological record may reflect the unusual character of the excavation mechanism rather than the frequency of such metamorphisms, and it may be expected that many similar terrains continue to reside near the base of the modern day continental crust.

**Acknowledgements.** This study originated as an M.Sc. project at Leeds University, while one of us (FBN) was in receipt of a Natural Environment Research Council studentship. Dr. P.H. Nixon is thanked for providing the sample material from the Labwor Hills for this project and for his comments on an earlier draft of the manuscript. Thanks are also due to Dr. P Treloar for access to the electron microprobe facilities at the Department of Earth Sciences, Cambridge University, and to Drs. B.J. Hensen and D.J. Ellis for reviewing the manuscript. Sandiford's research was supported by a University of Melbourne Research Promotion Grant.



## References

- Annersten H, Seifert F (1981) Stability of the assemblage orthopyroxene-sillimanite-quartz in the system  $\text{MgO}-\text{FeO}-\text{Fe}_2\text{O}_3-\text{Al}_2\text{O}_3-\text{SiO}_2-\text{H}_2\text{O}$ . *Contrib Mineral Petrol* 77:158-165
- Arima M, Barnett RL (1984) Sapphirine bearing granulites from Sipiwek Lake area of the late Archaean Pikwitonei granulite terrain, Manitoba, Canada. *Contrib Mineral Petrol* 88:102-112
- Baldock JW, Clark L, Reedman AJ, Wren AE (1969) Explanation of the geology of sheet 25 (Labwor Hills). Geological Survey Mines department Report 14, Republic of Uganda, p 37
- Bard JP (1983) Metamorphism of an obducted island arc: example of the Kohistan sequence (Pakistan) in the Himalayan collided range. *Earth Planet Sci Lett* 65:133-144
- Berg JH, Wheeler EP (1976) Osumilite of deep seated origin in the contact aureole of the anorthositic Nain Complex, Labrador. *Am Mineral* 61:29-37
- Bogdanova NG, Trovena NV, Zaborovskaya NB, Sukhanov MK, Berkhin SI (1980) The first find of metamorphic osumilite in the U.S.S.R. (in Russian). *Dok Akad Nauk Uzb SSR* 250:690-693
- Clifford TN (1975) Review of African granulites. *geol Soc Am Spec Pap* 156:49 pp
- Coward MP, Jan MQ, Rex D, Tarney J, Thirwell M, Windley BF (1982) Geo-tectonic framework of the Himalaya of N Pakistan. *J Geol Soc London* 139:229-308
- Dallwitz WB (1968) Co-existing sapphirine and quartz in granulite from Enderby Land, Antarctica. *Nature* 219:476-477
- Deer WA, Howie RA, Zussman J (1978) Rock forming minerals. Volume 2A: Single chain silicates. Longman, London
- Droop GTR, Bucher-Nurminen K (1984) Reaction textures and metamorphic evolution of sapphirine-bearing granulites from the Gruf Complex, Italian Central Alps. *J Petrol* 25:766-803
- Ellis DJ (1980) Osumilite-sapphirine-quartz granulites from Enderby Land: P-T conditions of metamorphism, implications for garnet-cordierite equilibria and the evolution of the deep crust. *Contrib Mineral Petrol* 74:201-210
- Ellis DJ, Green DH (1985) Garnet forming reactions in mafic granulites from Enderby Land, Antarctica - Implications for Geothermometry and Geobarometry. *J Petrol* 26:633-662
- Ellis DJ, Sheraton JW, England RN, Dalwitz WB (1980) Osumilite-sapphirine-quartz granulites from Enderby Land, Antarctica - mineral assemblages and reactions. *Contrib Mineral Petrol* 72:353-367
- England PC, Bickle M (1984) Continental thermal and tectonic regimes during the Archaean. *J Geol* 92:353-367
- Grew ES (1982) Osumilite in the sapphirine-quartz terrane of Enderby Land, East Antarctica: implications for osumilite petrogenesis in the granulite facies. *Am Mineral* 67:762-787
- Harley SL (1984) An experimental study of the partitioning of Fe and Mg between garnet and orthopyroxene. *Contrib Mineral Petrol* 86:359-373
- Harley SI (1985) Garnet-orthopyroxene bearing granulites from Enderby Land, Antarctica. Metamorphic pressure-temperature-time evolution of the Archaean Napier Complex. *J Petrol* 26:819-856
- Hensen BJ (1971) Theoretical phase relations involving cordierite and garnet in the system  $\text{MgO}-\text{FeO}-\text{Al}_2\text{O}_3-\text{SiO}_2$ . *Contrib Mineral Petrol* 33:191-214
- Hensen BJ (1977) The stability of osumilite in high grade metamorphic rocks. *Contrib Mineral Petrol* 64:197-204
- Hensen BJ (1986) Theoretical phase relations involving cordierite and garnet revisited: the influence of oxygen fugacity on the stability of sapphirine and spinel in the system  $\text{Mg}-\text{Fe}-\text{Al}-\text{Si}-\text{O}$ . *Contrib Mineral Petrol* 92:362-367
- Hensen BJ, Green DH (1971) Experimental study of the stability of cordierite and garnet in pelitic compositions at high pressures and temperatures I. Compositions with excess aluminosilicate. *Contrib Mineral Petrol* 33:309-330
- Hensen BJ, Green DH (1972) Experimental study of cordierite and garnet in Pelitic compositions at high pressures and temperatures II. Compositions with excess aluminosilicate. *Contrib Mineral Petrol* 35:331-354
- Lachenbruch AH, Sass JH (1978) Models of an extending lithosphere and heat flow in the Basin and Range province. *Geol Soc Am Mem* 152:209-250
- Lindsley DH (1976) Experimental studies on oxide minerals. In: Rumble D (ed) *Oxide minerals*. Mineral Soc Am Short Course Notes: 101-300
- Maijer C, Jansen JBH, Wevers J, Poorter RPE (1977) Osumilite, a mineral new to Norway. *Nor Geol Tidsskr* 57:187-188
- Morse SA, Talley JH (1971) Sapphirine reactions in deep-seated granulites near Wilson Lake, Central Labrador, Canada. *Earth Planet Sci Lett* 10:325-328
- Newton RC (1972) An experimental determination of the high pressure stability limits of cordierite under wet and dry conditions. *J Geol* 80:398-420
- Newton RC, Charlu TV, Kleppa OJ (1974) A calorimetric investigation of the high pressure stability of anhydrous magnesium cordierite with application to granulite facies metamorphism. *Contrib Mineral Petrol* 44:25-311
- Newton RC, Perkins D (1982) Thermodynamic calibration of geobarometers based on the assemblage garnet-plagioclase-orthopyroxene (clinopyroxene)-quartz. *Am Mineral* 67:203-222
- Nixon PH, Reedman AJ, Burns LK (1973) Sapphirine bearing granulites from Labwor, Uganda. *Mineral Mag* 39:420-428
- Nixon PH, Grew ES, Condliffe E (1984) Kornerupine in a sapphirine-spinel granulite from Labwor Hills, Uganda. *Mineral Mag* 48:550-552
- Putnis A, Holland TJB (1986) Sector trilling in cordierite and equilibrium overstepping in metamorphism. *Contrib Mineral Petrol* 93:265-272
- Richardson SH, Gurney JJ, Erlank AJ, Harris JW (1984) Origin of diamonds in old enriched mantle. *Nature* 310:198-202
- Sahama THG, Lehtinen M, Rehtijärvi P (1974) Properties of sapphirine. *Ann Acad Sci Fenn, Ser A* 3 114:1-23
- Sandiford M (1985) The metamorphic evolution of granulites at Fyfe Hills; implications for Archaean crustal thickness in Enderby Land, Antarctica. *J Meteorol Geol* 3:155-178
- Sandiford M, Powell R (1986a) Pyroxene exsolution in granulites from Fyfe Hills, Enderby Land, Antarctica: evidence for 1,000 °C temperatures in Archaean continental crust. *Am Mineral* 71:946-954
- Sandiford M, Powell R (1986b) Deep crustal metamorphism during continental extension: ancient and modern examples. *Earth Planet Sci Lett* 79:151-158
- Schreyer W, Seifert F (1967) Metastability of an osumilite end member in the system  $\text{MgO}-\text{FeO}-\text{Fe}_2\text{O}_3-\text{Al}_2\text{O}_3-\text{SiO}_2-\text{H}_2\text{O}$  and its possible bearing on the rarity of natural osumilites. *Contrib Mineral Petrol* 14:343-358
- Shackleton RM (1986) Precambrian collision tectonics in Africa. In: *Collision tectonics* Geological Society Special Publication No 19:329-349
- Sheraton JW, Offe LA, Tingey RJ, Ellis DJ (1980) Enderby Land, Antarctica - an unusual Precambrian high grade terrain. *J Geol Soc Aust* 27:1-18
- Thompson AB (1981) The pressure temperature (P,T) plane as viewed by geophysicists and petrologists. *Terra Cognita* 1:11-20
- Warren RG (1983) Metamorphic and tectonic evolution of granulites, Arunta Block, Central Australia. *Nature* 305:300-303
- Wells PRA (1980) Thermal models for magmatic accretion and subsequent metamorphism of continent crust. *Earth Planet Sci Lett* 46:253-265